Peer reviewed version

Link to published version (if available):
10.2514/6.2017-3716

Link to publication record in Explore Bristol Research
PDF-document

University of Bristol - Explore Bristol Research
General rights

On the Application of Trailing-edge Serrations for Noise Control from Tandem Airfoil Configuration

Xiao Liu,[*] Syamir Alihan Showkat Ali,[†] Mahdi Azarpeyvand[‡]

Faculty of Engineering, University of Bristol, BS8 1TR, UK

This paper presents a preliminary study on the application of serrations as a passive control method for reducing the aerodynamic sound from airfoils in tandem. The aim of the study is to investigate the effectiveness of serrated trailing-edge on cambered NACA 65-710 tandem airfoil to control and regularize the turbulent flow within the gap area between the two airfoils. The wake flow characteristics for a cambered NACA 65-710 airfoil with and without the serration treatment have been quantified using two-dimensional Particle Image Velocimetry (PIV). To better understand the aerodynamic and aeroacoustics effects of serrations on the tandem configuration, the rear airfoil was equipped with several pressure taps and surface pressure transducers. The surface pressure coefficient distributions and surface pressure fluctuations have been measured using the pressure taps and remote sensing probe technique. Experiments were performed using a sharp sawtooth serration, for a number of tandem airfoil configurations, with different airfoil separation distances. The results show that the use of serrations at relatively high angles of attack, namely 10 and 15 degree, can lead to a significant reduction of the turbulent kinetic energy, which is believed to be due to the interaction between the flow field at the tip and root of the serrations. Results have also shown that a significant reduction of surface pressure fluctuation can be achieved over the leading-edge area of the rear airfoil, particularly for configurations at high angles of attack. The wake and surface pressure results have confirmed that the use of serrated trailing-edges can lead to robust control of the wake flow and reduction of wake interaction noise.

Nomenclature

AoA	angle of attack, deg
α_s	serration angle, deg
α_{front}	angle of attack of front airfoil, deg
α_{rear}	angle of attack of rear airfoil, deg
λ	serration wavelength, mm
$2h$	amplitude of serration, mm
d	slot width, mm
H	slot depth, mm
Re_c	chord-based Reynolds number
U	streamwise flow speed, m/s
U_0	free-stream wind speed, m/s
W	gap distance between the front and rear airfoils, mm
W_x	streamwise distance between the center-points of the airfoils, mm
W_y	vertical distance between the center-points of the airfoils, mm
C_p	pressure coefficient, $p\text{-}p_o/q_o$
$C_{p'_{rms}}$	fluctuating pressure coefficient, p'_{rms}/q_o

[*]Ph.D Student, Faculty of Engineering, `xiao.liu@bristol.ac.uk`

[†]Ph.D Student, Faculty of Engineering, `ss14494@bristol.ac.uk`

[‡]Senior Lecturer and Royal Academy of Engineering Research Fellow, Mechanical Engineering, `m.azarpeyvand@bristol.ac.uk`

American Institute of Aeronautics and Astronautics

p'_{rms}	root-mean-square pressure fluctuation, Pa
p_o	free-stream static pressure, Pa
q_o	free-stream dynamic pressure, kg/ms^2
TKE	turbulent kinetic energy, $1/2((u'_{rms})^2 + (v'_{rms})^2)$, m^2/s^2
u'_{rms}	root-mean-square streamwise velocity fluctuation, m/s
v'_{rms}	root-mean-square lateral velocity fluctuation, m/s

I. Introduction

The aerodynamic noise produced by the rotating blades has been studied over the past decades. The noise from rotating blades, as a component of compressors and turbines, caused as a result of the interaction of turbulent flow from the front-blade with the rear-blade, has remained a challenging task. The noise generation mechanism of contra-rotating open rotor (CROR) propulsion systems has also attracted much research interest in the recent years.[1] It has been shown that the interaction of the tip and wake flow caused by the front propeller with the rear blades is a major source of noise and therefore reduction of the front-blade wake turbulence intensity can significantly reduce the overall noise signature of the CROR system. The noise from rotating blades in a uniform flow can be generally categorised as trailing-edge noise, early separation and stall noise.[2] The reduction of blade trailing-edge noise has been investigated extensively over the past decade. To reduce trailing-edge noise, several passive methods such as serrated trailing-edge,[3–15] porous surface treatments,[16–19] surface treatments,[20,21] brushes[22,23] and morphing[24,25] have been under investigation. Amongst all the other passive trailing-edge treatments, serrated trailing-edges, in particular, have received considerable interest due to its simple yet efficient noise reduction capabilities.

The efficiency of serrations for assessing the trailing-edge noise have been extensively investigated by Howe.[26–28] A detailed analytical studies by Howe have shown that the trailing-edge noise can be reduced significantly by applying sawtooth and sinusoidal serrations to the trailing-edge, which introduce the destructive sound interference. It is also claimed that this sound interference enables the breakdown the lateral correlation length of the turbulence structure near the trailing-edge, leading to a noticeable noise reduction. It has been also shown that the magnitude of noise reduction relies upon the frequency, spanwise spacing and length of the serration teeth. Howe showed that the optimal attenuation of noise can be accomplished with trailing-edge sharpness of larger than 45°. However, Howe's mathematical model does not match the absolute noise reduction with the experimental data. Lyu's et al.[29,30] recent analytical model improved the existing model developed by Howe by taking into account the existence of constructive sound interference in addition to the destructive sound interference predicted by Howe, and the results have shown a better agreement with the experimental data. Recent studies have shown that the implementation of trailing-edge serrations, such as sawtooth and slotted-sawtooth serrations, which have superior noise reduction efficiency,[13] can also significantly reduce the wake turbulence intensity, particularly at high angles, where maximum aerodynamic performance is obtained.[7–9] This significant faster turbulent energy decay within the wake region is believed to be due to the three-dimensional flow originating from the serration tip and root planes. The possibility of reducing the turbulence level using serrations shows an option for a new technique for reducing noise generated by wake-airfoil interaction, such as contra-rotating propellers, rotor-stator configuration, etc.

To expand the existing knowledge and better understand the effect of using serrations on the aerodynamic and acoustic performance of airfoils in tandem, detailed study of the wake development and surface pressure fluctuations have been carried out and presented in this paper. A comprehensive aerodynamic study using a cambered NACA 65-710 airfoil with and without trailing-edge serration has been carried out using the two-dimensional Particle Image Velocimetry (PIV) technique. Thorough measurements have been also carried out for pressure coefficient distributions on the rear airfoil. The effect of serrations on the noise generation for the tandem NACA 65-710 configuration has also been studied by studying the surface pressure fluctuations on the rear airfoil using the remote sensing probe method. The experimental setup manufactured for the present study and the aerodynamic measurement techniques are discussed in section II. The results and discussions are provided in section III.

II.   Experimental Setup

Experiments were carried out on tandem cambered asymmetrical NACA 65-710 airfoil in the low turbulence closed-circuit wind tunnel of the University of Bristol. The tunnel has an octagonal working section of $0.8m \times 0.6m \times 1m$, with contraction ratio of $12:1$ and capable of reaching reliable speeds of up to $100~m/s$, with turbulent intensity of 0.05%. The inflow velocity used for this study is $30~m/s$.

A.   Airfoil and Serration Model Design Setup

The schematic of the tandem airfoils configuration with and without the trailing-edge serrations are shown in Fig. 1. The front and rear airfoils were manufactured from aluminium-7075 and RAKU-TOOL WB-1222 polyurethane board, respectively and machined using a computer numerical control (CNC) machine. The front airfoil was designed with a $2.3~mm$ blunt trailing-edge with a $15~mm$ depth and $0.8~mm$ thick slot along the span of the airfoil in order to install the flat plate (baseline) and serration inserts at the trailing-edge (see Figs. 1(a) and (c)). The rear airfoil, on the other hand, was equipped with a total number of 34 surface pressure taps on both the pressure and suction sides of the airfoil, see Figs. 1(b) and (d). The two airfoils are placed parallel to each other, in a uniform flow, and rectangular end-plates with a chamfered leading-edges were used to maintain a nearly two-dimensional flow over the two airfoils.

In the present work, the sawtooth serrations (Fig. 2(a)) were chosen based on their turbulent kinetic energy and noise reduction performance from the previous experimental studies.[7-9] The geometrical parameters of the serrations used in this study, namely the amplitude $(2h)$, periodicity wavelength (λ) and the angle of serration edge (α_s), are provided in Table 1. The geometrical parameters of the tandem airfoil configuration (Fig. 2(b)), such as the gap distances between the front and rear airfoils (W), the streamwise distance between the centre-points of the airfoils (W_x), vertical distance between the airfoils centre-points (W_y), angle of attack of front airfoil (α_{front}) and rear airfoil (α_{rear}) are given in Table 2. Note that, W_x and W_y were defined based on the the locations where the the maximum turbulent kinetic energy is observed from the PIV results obtained for the baseline case of an isolated NACA 65-710 airfoil.
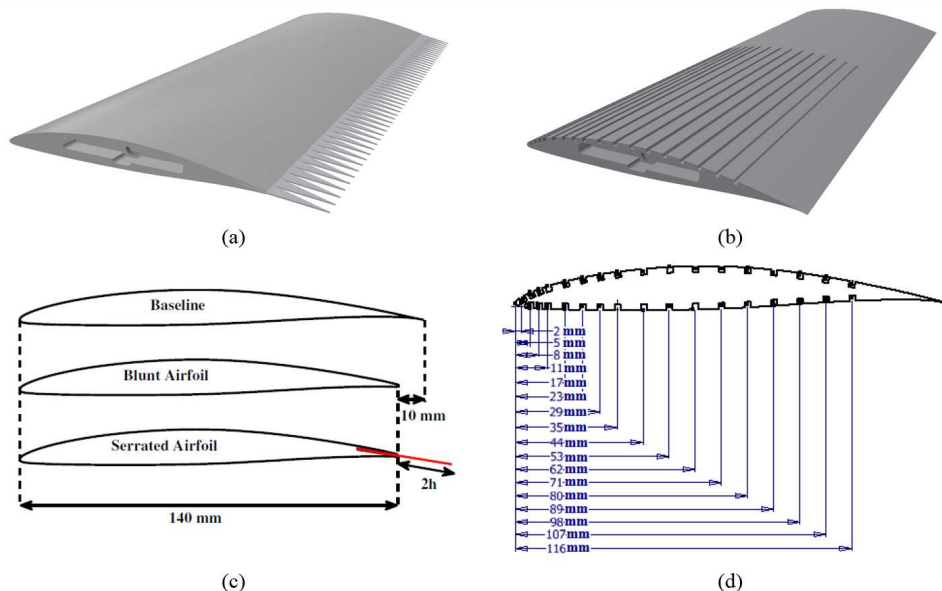

Figure 1:   Tandem airfoil configuration, (a) Front airfoil model: Assembly view of NACA 65-710 with trailing-edge serration, (b) Rear airfoil model: NACA 65-710 with pressure taps distribution, (c) NACA 65-710 with and without trailing-edge serration, (d) NACA 65-710 and the locations of the pressure taps
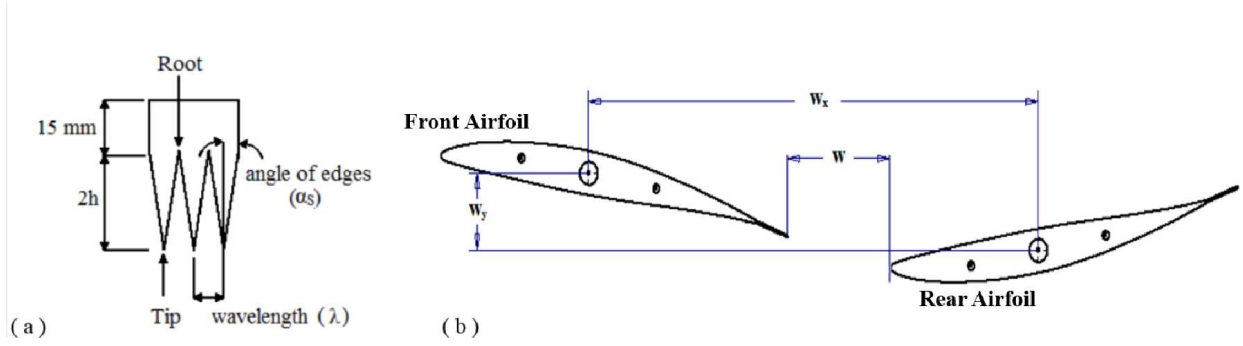
Figure 2: (a) Trailing-edge treatment: Sawtooth serration, (b) Tandem airfoil setup

Table 1: Geometrical parameters of trailing-edge treatments

Cases	Treatments	$2h$	λ	λ/h	α_s
		mm	mm		degrees
Case 1	Blunt	0	-	-	-
Case 2	Baseline	15	-	-	-
Case 3	sawtooth	30	9	0.6	8.53

Table 2: Tandem airfoil setup parameters

Cases	α_{front} degrees	α_{rear} degrees	W	W_x mm	W_y mm
Case 1	5	5	$0.3c$	199.106	19.113
Case 2	5	5	$0.5c$	229.106	25.113
Case 3	5	5	$1.0c$	304.106	37.113
Case 4	10	10	$0.3c$	197.307	36.368
Case 5	10	10	$0.5c$	227.307	30.868
Case 6	10	10	$1.0c$	302.307	42.368
Case 7	15	15	$0.3c$	194.349	-0.998
Case 8	15	15	$0.5c$	224.349	-0.998
Case 9	15	15	$1.0c$	299.349	2.752

B.   Particle Image Velocimetry Setup

The wake development and the energy content study of the front airfoil with and without the trailing-edge serration were carried out using a two-component Particle Image Velocimetry (PIV). A Dantec DualPower $200mJ$ Nd:YAG laser with a wavelength of $532\ nm$ was used to produce $1\ mm$ thick laser sheet with the time interval between each snapshots of $23\ \mu s$ and a repetition rate of 2.5 Hz. A mixture of Polyethylene glycol 80 with a mean diameter of $1\ \mu m$ was used to seed the air inside the low turbulence wind tunnel. A total number of 1600 images for each measurement were captured using a FlowSense EO 4M CCD camera with a resolution of 2072×2072 pixels and 14 bit, corresponding to field view of $14.8\ cm \times 14.8\ cm$. The images were analysed with the DynamicStudio software from Dantec. The iterative process yield grid correlation window of 16×16 pixels with an overlap of 50 %, resulting in a facial vector spacing of $0.43\ mm$.

C. Surface Pressure Measurement Setup

The steady and unsteady surface pressure measurements have been carried out using the MicroDaq pressure scanner and remote sensing probes on both sides of the rear airfoil, see Fig 1. The pressure taps for pressure coefficient distributions were made from 1.6 mm diameter brass tubing with 0.4 mm pinholes with the angle perpendicular to the surface of the airfoil to avoid any aerodynamic interference between the pressure taps. The surface pressure fluctuations measurements are performed using remote sensing probes, which are connected between the brass tube of the pressure tap to a remote microphone holder equipped with 34 Panasonic WM-61A microphones using plastic tubing with the inner and outer diameter of 0.8 mm and 3.6 mm, see Fig. 3. The detailed description of the remote sensing probe methodologies and framework will be documented in a separate paper. The data was acquired by a National Instruments PX1e-4499 at a sampling rate of 2^{16} Hz and sampling time of 8 seconds, and processed using the Matlab software.
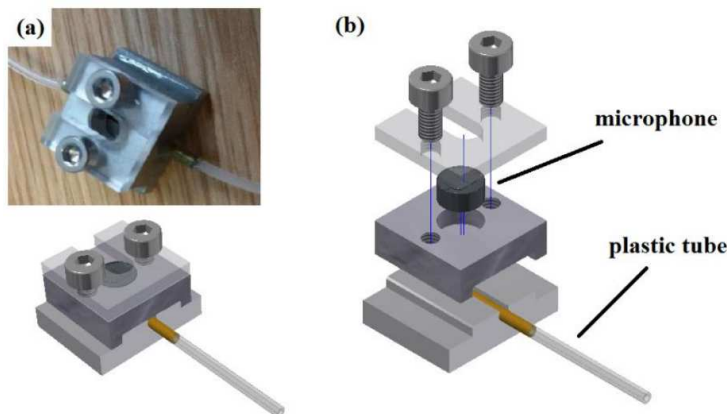

Figure 3: (a)Schematic drawing of remote sensing probe, (b)Remote sensing assembly drawing

III.   Results and Discussion

A.   NACA 65-710 Airfoil Wake Measurements

To better understand the effects of serration on the wake development of the airfoil, the flow measurements of NACA 65-710 airfoil for the baseline, blunt and sawtooth serration ($\lambda = 9mm$) configurations have been carried out using Particle Image Velocimetry. The wake measurements were performed at angles of attack, AoA = 0°, 5°, 10° and 15° for chord-based Reynolds number of $Re_c = 3 \times 10^5$, corresponding to the flow velocity of $U_0 = 30$ m/s. The wake profiles were captured at downstream locations, x=0.2c to 0.8c relative to the trailing-edge of the baseline case. The wake results are only presented for the AoA = 5°, 10° and 15°, where the results were found to show significant changes in the velocity profile and turbulent kinetic energy (TKE) with the implementation of trailing-edge serration.

Figure 4 shows the wake velocity profile and turbulent kinetic energy (TKE) results at AoA = 5°. In the near wake region ($x/c = 0.2$ and 0.3), the wake velocity profiles at the tip position of the sawtooth serration are similar to that of the baseline, but the root-flow exhibits a smaller velocity deficit, with the deficit dip location moved upward along the vertical plane. It is also clear that the wake velocity deficit for both the tip- and root-flow at the far-wake locations ($x/c = 0.5$ to 0.8) exhibits an overall upward deflection of the flows compared to the baseline case. It can also be observed that at the vicinity of the airfoil trailing-edge ($x/c = 0.2$ and 0.3), there is a noticeable reduction in the TKE magnitude of both the tip and root cases compared to that of the baseline. Also, the TKE peak positions have shifted upward for the root-flow and slightly downward for the tip-flow relative to the baseline case, signifying the existence of a strong upward flow through the serration valleys.

The wake velocity profiles and TKE results at AoA = 10° and 15° with and without trailing-edge serrations are presented in Figs. 5 and 6, respectively. It can be seen that at AoA = 10°, the velocity profiles for sawtooth-serration has a smaller velocity deficit, especially for the root-flow case in the near-wake region,

$x/c = 0.2$ to 0.4. The resultant flow after mixing for the tip- and root-flows has a similar trend compared to the baseline flow but a significant downward deflection compared to the blunt case. A significant reduction in the TKE can be observed for both the tip- and root-planes, by up to 49 % in the near wake region, and more at the far wake locations. It can be concluded that the use of trailing-edge serration at AoA = 10° can significantly modify the wake structure by reducing the velocity deficit in the near wake region, leading to a major TKE decay which is believed to be due to the interaction between the tip- and root-flow planes. The results obtained here are found to be in good agreement with those obtained by Liu et al.[31]

From the velocity profiles at AoA = 15° presented in Fig. 6 for the near-wake region ($x/c = 0.2$ to 0.4), it can be seen that the tip- and root-flow velocity decreases significantly on the airfoil's upper surface ($y/c > 0$). It can be observed that both the baseline and serration cases exhibit a large velocity wake-width, indicating to an early separation on the airfoil's suction side. The velocity results show that the wake deficit dip location for both the tip- and root-flow are located slightly below the dip location of the baseline airfoil. The TKE increases for the root-flow case in the near-wake location ($x/c = 0.2$) above the trailing-edge compared to that of baseline, which can be associated to the interaction between the flow field at the tip and root of the serrations. Results have also shown that reduction in TKE of up to 28% above the airfoil and 48% below the airfoil can be obtained at far-wake locations ($x/c = 0.5$ to 0.7), where the magnitude of TKE reduction was higher relative to the near-wake locations. The serration velocity and TKE profiles eventually coincide to that of the baseline case at $x/c = 0.8$.

It can be concluded that the use of serrations at relatively high angles of attack, especially for the AoA = 10°, can lead to significant changes to the velocity profile and reduction of the turbulent kinetic energy (TKE). The results demonstrated here are particularly important in the context of wake-interaction noise and the possibility of noise reduction in tandem airfoil configuration by stabilizing the wake flow using trailing-edge serrations. A detailed analysis of the possibility of reducing wake interaction noise will be presented in the next sections by studying the surface pressure coefficients and surface pressure fluctuations over the rear airfoil.
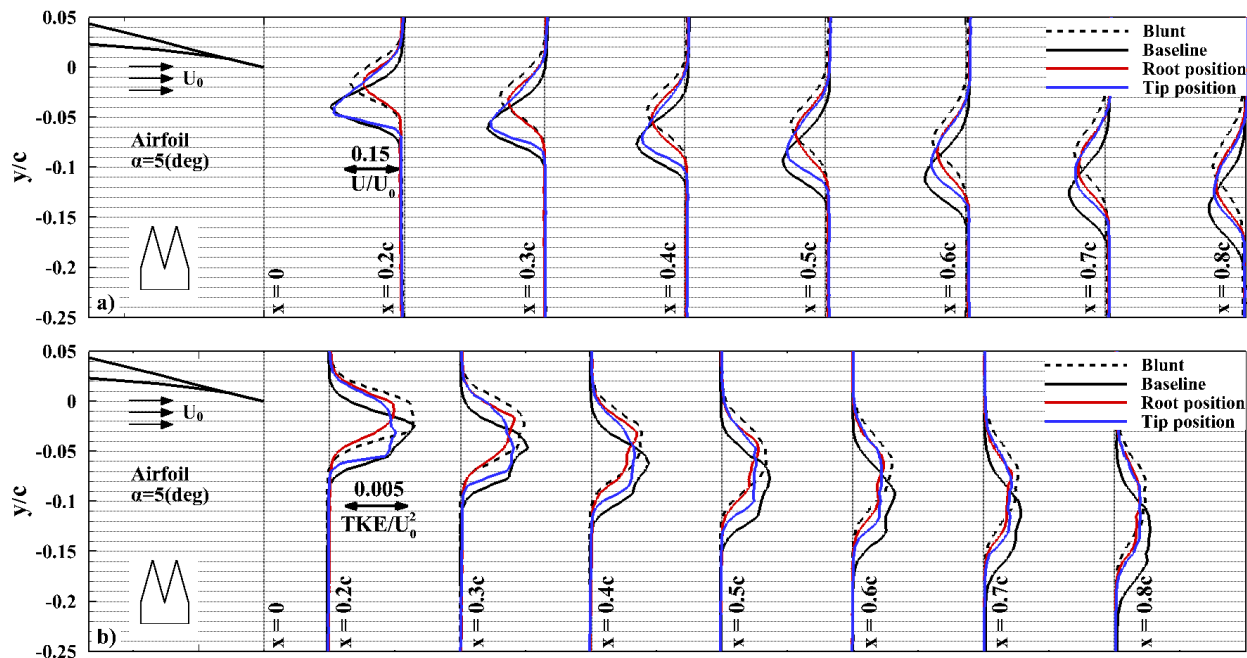

Figure 4: Wake development for NACA 65-710 at $\alpha = 5°$, (a) mean velocity profile and (b) turbulent kinetic energy
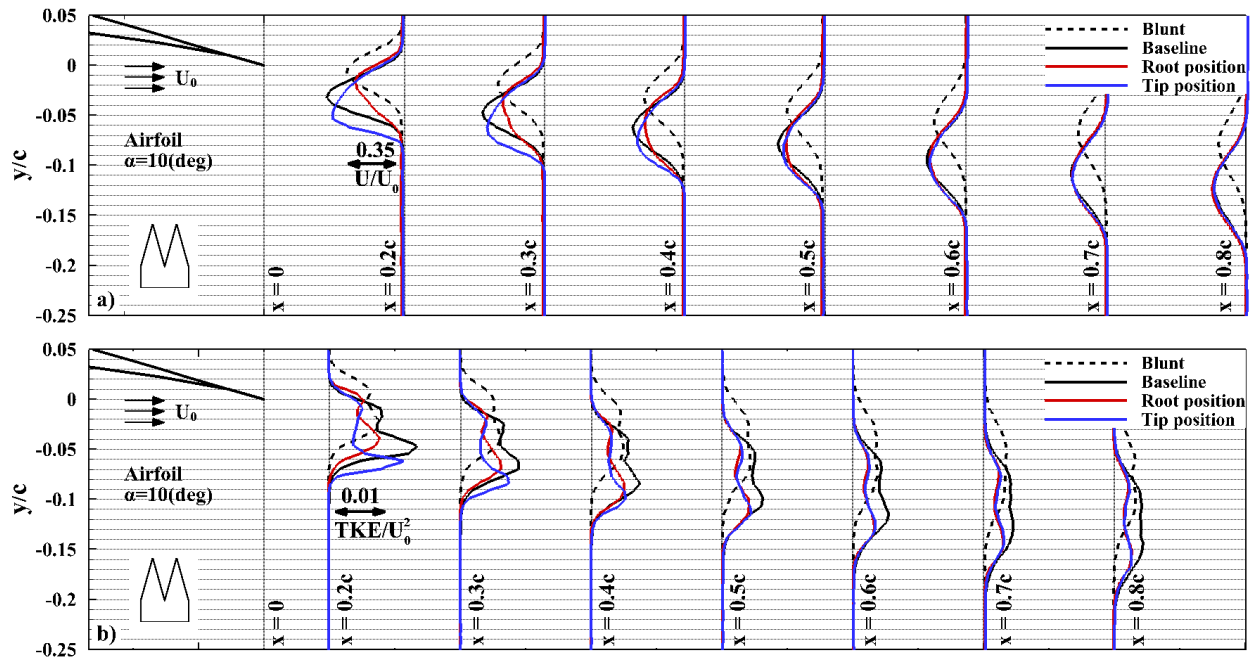
American Institute of Aeronautics and Astronautics

Figure 5: Wake development for NACA 65-710 at $\alpha = 10°$.

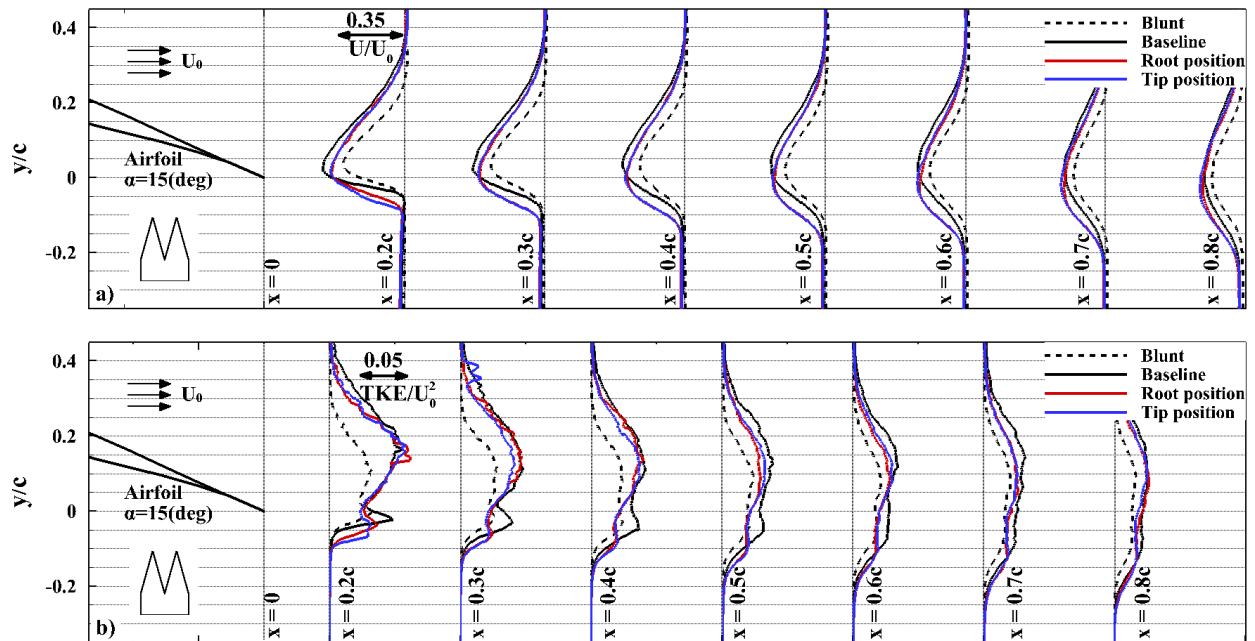
Figure 6: Wake development for NACA 65-710 at $\alpha = 15°$.

B. Pressure Coefficient Distribution

The steady and unsteady surface pressure distributions along the rear NACA 65-710 airfoil for baseline and the tip and root serrated cases have been examined. The mean C_p and fluctuating $C_{p'_{rms}}$ pressure coefficients of the rear airfoil at angles of attack, AoA = 5°, 10° and 15°, with the airfoil separation distance of $W = 0.3c$, $0.5c$ and $1.0c$ are shown in Figs. 7 and 8. At low angle of attack, AoA = 5°, it can be seen that the mean
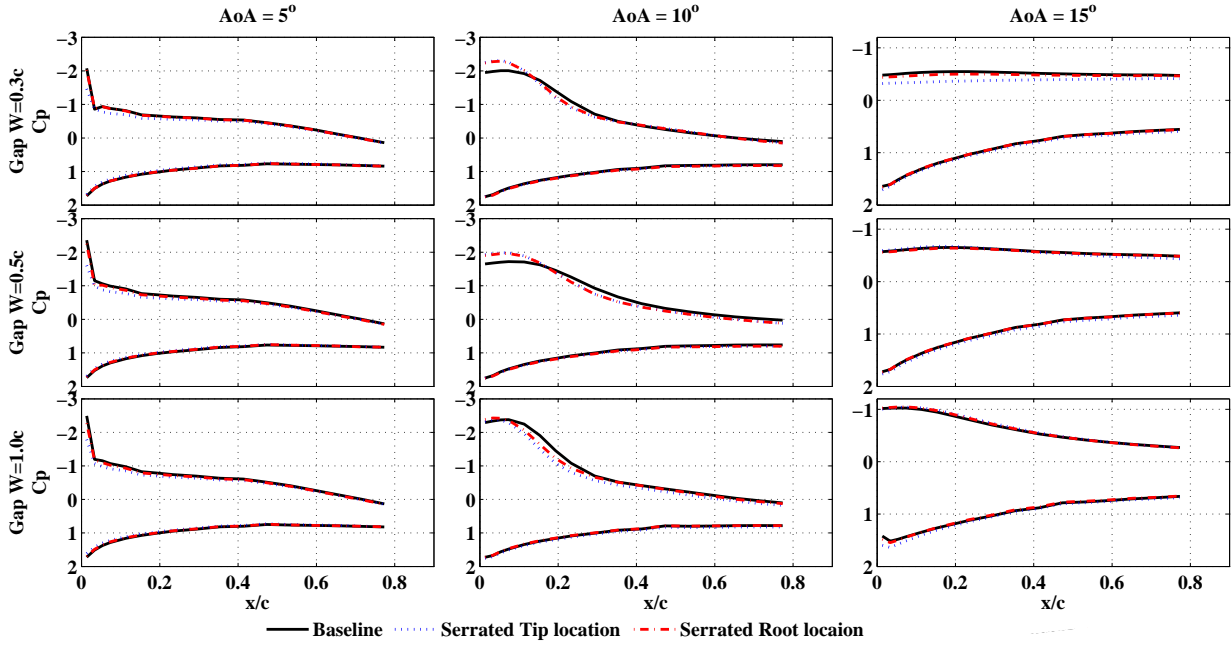
Figure 7: Mean pressure coefficients (C_p) for baseline and serrated NACA 65-710 airfoils at AoA = 5°, 10°, 15°, at $U_0 = 30$ m/s with airfoil separation distance of W = $0.3c$, $0.5c$ and $1.0c$
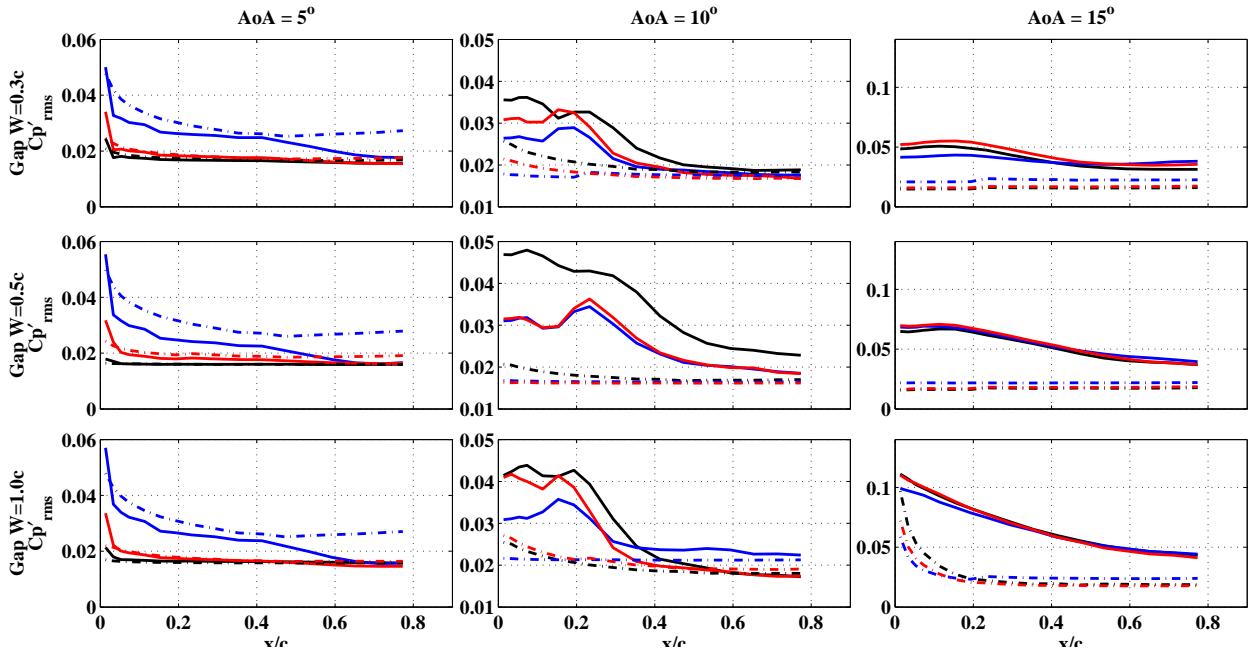

Figure 8: RMS pressure coefficients ($C_{p'_{rms}}$) for baseline and serrated NACA 65-710 airfoils at AoA = 5°, 10°, 15°, at $U_0 = 30$ m/s with airfoil separation distance of W = $0.3c$, $0.5c$ and $1.0c$, solid line: suction side of the rear airfoil, dashed line: pressure side of the rear airfoil

pressure coefficient, C_p is slightly reduced on the suction side of the airfoil (upper surface) for serrated cases (tip and root positions) for all airfoil gap distances, while on the pressure side (lower surface), there is only

American Institute of Aeronautics and Astronautics

a little difference between the baseline and serrated cases. Interestingly, there is a significant change in the C_p distribution at the airfoil suction side for AoA = 10°. At AoA = 10°, with W = 0.3c, 0.5c, the C_p increases in the near leading-edge region ($x/c < 0.15$) and reduces significantly further downstream of the leading-edge over the airfoil suction side, particularly for the gap distance of W = 0.5c. Comparison of the gaps between the tandem airfoils show that the larger gap (W = 1.0c), at AoA = 10° on the suction side has a small increase in the near leading-edge ($x/c < 0.1$), but a significant reduction in the region up to 0.3c. Nonetheless, the results obtained for the pressure side of the airfoil for all gap distances remained similar for both the baseline and serrated cases. For higher angle of attack, AoA = 15°, W = 0.3c, a noticeable reduction in C_p can be seen on the suction side of the airfoil for the serrated cases. At W = 0.5c, only a mild change in C_p can be observed on both the suction and pressure sides of the airfoil for the serrated cases. However, at W = 1.0c, the C_p at the airfoil suction side shows a slight increase for the serrated cases over half of the chord distance whereas over the pressure side, the C_p drops a little, especially in the near leading-edge locations. The $C_{p'_{rms}}$, on the other hand, is significantly reduced for the serrated cases at high angles of attack on the suction side of the airfoil, especially for AoA = 10°, which is associated with low level of turbulence intensities downstream of the front airfoil. Lower turbulence kinetic energy levels yield lower rms pressure coefficients, which is also consistent with the results obtained in Figs. 5 and 6. The pronounced changes of C_p and $C_{p'_{rms}}$ in the serrated cases are likely to be due to the lower wake-turbulent interaction between the tandem airfoils, where the serrated case has noticeably reduced the turbulent kinetic energy downstream of the front airfoil. To further expand the results obtained for surface pressure distributions, a detailed study of the surface pressure fluctuations are discussed in the next section.

C.   Surface Pressure Fluctuations

In order to further investigate the effectiveness of serration treatments for reducing aerodynamic loading and noise, surface pressure fluctuation measurements have been performed on the rear airfoil using the remote sensing probe method. The results are presented for the AoA = 10° and 15°, based on the significant TKE reduction results observed in Figs. 5 and 6. Figures 9 and 10 present the surface pressure fluctuations (ϕ_{pp}) results for the baseline and serrated tandem airfoil at AoA = 10° and 15°, respectively, with different horizontal gap distances (W=0.3c, 0.5c and 1.0c) between the airfoils, at x/c = 0.013, 0.053, 0.233 and 0.533 on both the suction (upper row) and pressure (bottom row) sides of the rear airfoil. For aerofoils at large angles of attack, the flow will separate from the aerofoil suction side and therefore, will contribute to noise generation. The pressure side, on the other hand, have negligible changes in the intensity of pressure fluctuations, which will not contribute to the radiated noise. In what follows, the results of surface pressure fluctuations with and without the serration treatments will be discussed briefly for the tandem configuration on the suction side of the rear airfoil.

At AoA = 10°, W = 0.3c, the intensity of pressure fluctuations in the near leading-edge region (x/c = 0.013) of the airfoil's suction side is almost negligible and increases slightly in the entire frequency region at x/c = 0.053 for the serrated case. However, at x/c = 0.233 and 0.533, the ϕ_{pp} of the serrated case reduces in the low fc/U_0 region and became similar to that of the baseline case at higher fc/U_0 region. The overall surface pressure fluctuations for the serrated case changes significantly when the gap distances between the airfoils increases. At AoA = 10°, W = 0.5c, a clear reduction in ϕ_{pp} can be seen at x/c = 0.013, 0.053 and 0.2333 on the suction side of the airfoil, in the low fc/U_0 region for the serrated case, but a slight increase of ϕ_{pp} can be seen in the higher fc/U_0 region in the near leading-egde locations and became similar to that of the baseline at x/c = 0.533. The results have also shown that a significant reduction of ϕ_{pp} on the suction side of the rear airfoil can be achieved with larger gap distance between airfoils (W = 1.0c), where a significant reduction of ϕ_{pp} is observed in the low frequency region for almost all the measurement locations (x/c = 0.013, 0.053 and 0.233). Contrary to the results obtained with smaller gap distances (W=0.3c and 0.5c), the pressure fluctuations obtained for the airfoils configuration with gap distance of W = 1.0c at higher frequencies became almost similar to that of the baseline in the near wake region (x/c = 0.013 and 0.053), but a noticeable reduction of ϕ_{pp} seen at x/c = 0.233. It is also seen that at further downstream locations from the leading-edge of the rear airfoil (x/c = 0.533), the pressure fluctuations of the serrated case is similar to that of the baseline case, which can be attributed to an early separation on the suction side of the airfoil.

Contrary to the findings obtained from the surface pressure fluctuations at AoA = 10°, the use of serration at high angles of attack, AoA = 15°, however, appears to have completely change the ϕ_{pp} at all the gap distances between the airfoils. The results depicted in Fig. 10 for the AoA = 15°, W = 0.3c show a significant reduction in ϕ_{pp} for all the measurement locations (x/c = 0.013, 0.053, 0.233 and 0.533), in the

entire frequency region, on the suction side of the rear airfoil. At $W = 0.5c$, a moderate reduction of ϕ_{pp} can still be seen in the near wake region ($x/c = 0.013$ and 0.053) for the serrated case on the suction side of the airfoil at low fc/U_0 region, but eventually converge to that of the baseline case at downstream locations from the airfoil leading-edge ($x/c = 0.233$ and 0.533). The results have also shown that there is no changes in the ϕ_{pp} between the serrated and baseline cases on the suction side of the rear airfoil with the larger gap distance, $W = 1.0c$ between the airfoils. This is believed to be due to the early separation of the flow on the suction side of the airfoil. The ϕ_{pp} observed on the pressure side of the baseline and serrated cases, remain nearly similar to each other, especially for the larger gap distance between the airfoils.

As demonstrated in the results obtained from Figs. 9 and 10, significant reduction of the surface pressure fluctuations especially at low frequencies in the near leading-edge locations of the rear airfoil can be achieved by using trailing-edge serrations on the front airfoil. Results have also shown that a significant reduction of surface pressure fluctuations can be achieved over the leading-edge area of the rear airfoil, particularly for configurations, at high angles of attack. This is believed to be due to the significant reduction in the energy content from the turbulent-wake flow structures within the gap. Also, it can be concluded that the reduction of the front-serrated trailing-edge airfoil wake turbulence intensity can significantly reduce the overall surface pressure fluctuations signature of the rear airfoil, especially in the near leading-edge locations.

IV.   Conclusion

The application of serration treatments from tandem airfoil as a method to control the wake development and hence the noise generation and radiation has been studied experimentally. Results of the flow analysis have shown that the mean velocity and the energy content of the wake flow can be reduced using the front airfoil serrated trailing-edge, especially at high angles of attack. It is also obvious that the use of trailing-edge serration on the front airfoil can lead to significant reduction of the surface pressure fluctuations over the near leading-edge region of the rear airfoil. Results have also shown that significant reduction in surface pressure fluctuations in the near leading-edge region, on the suction side of the rear airfoil can be achieved particularly with the tandem configurations at high angles of attack. The possibility of minimizing the unsteady aerodynamic loading on the rear airfoil and turbulence interaction between the airfoils using serration between the tandem airfoil can be interpreted as a potential control of the noise generation mechanism. In order to better understand the effect of trailing-edge serrations in the context of tandem airfoil configurations, further experiments, including the far-field noise measurements will be performed.
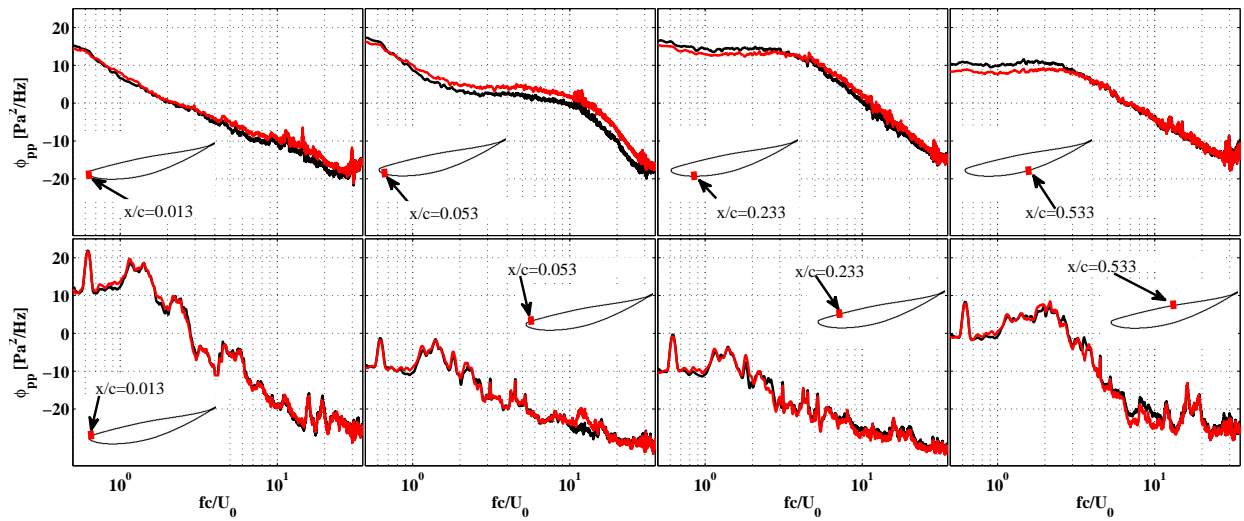
American Institute of Aeronautics and Astronautics

(a) Gap distance between the airfoils, $W = 0.3\ c$
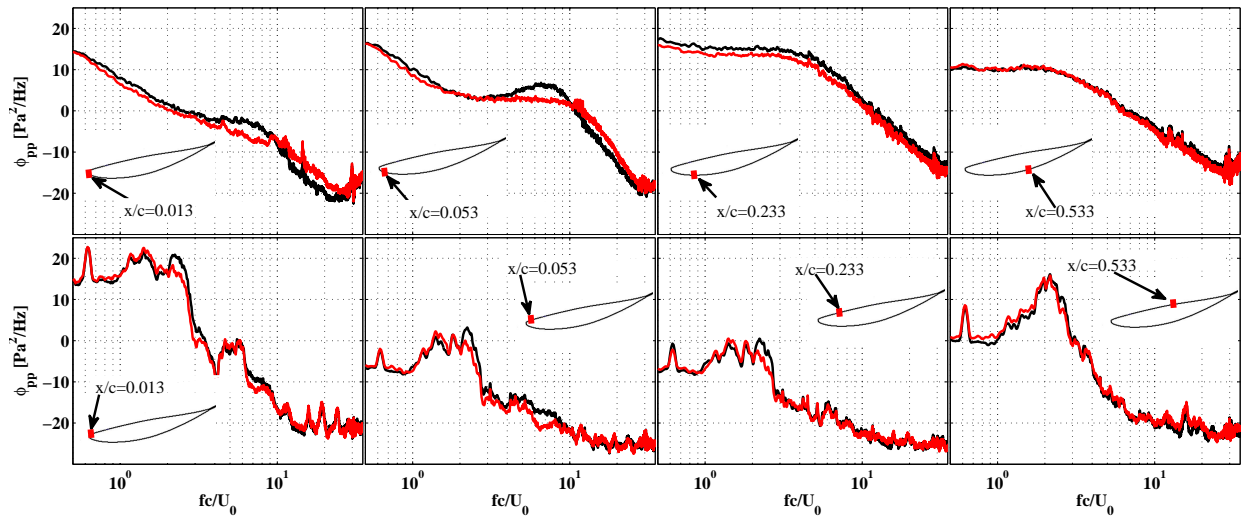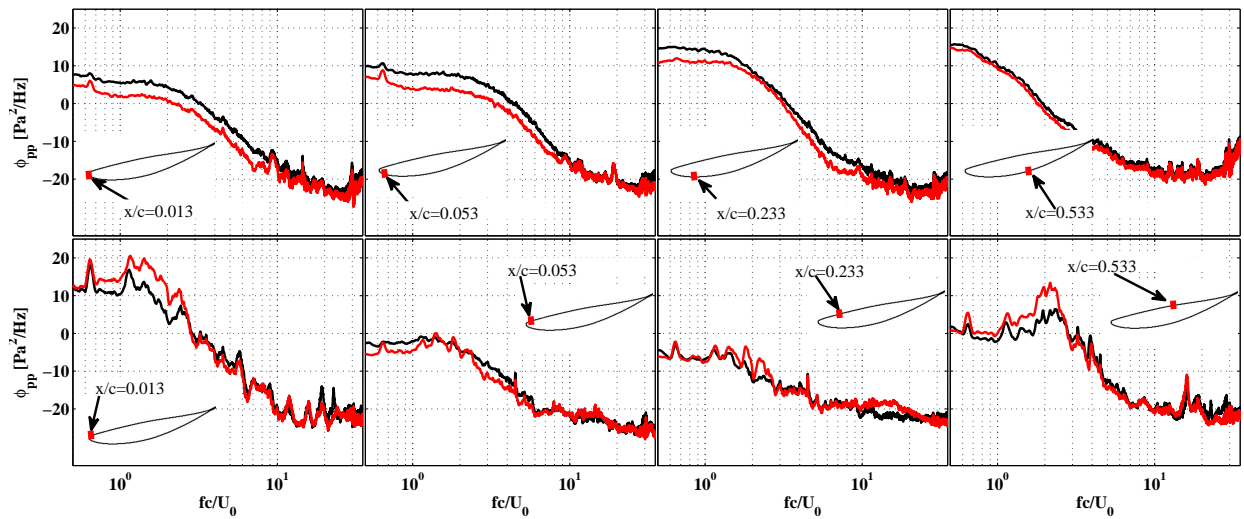

(b) Gap distance between the airfoils, $W = 0.5\ c$
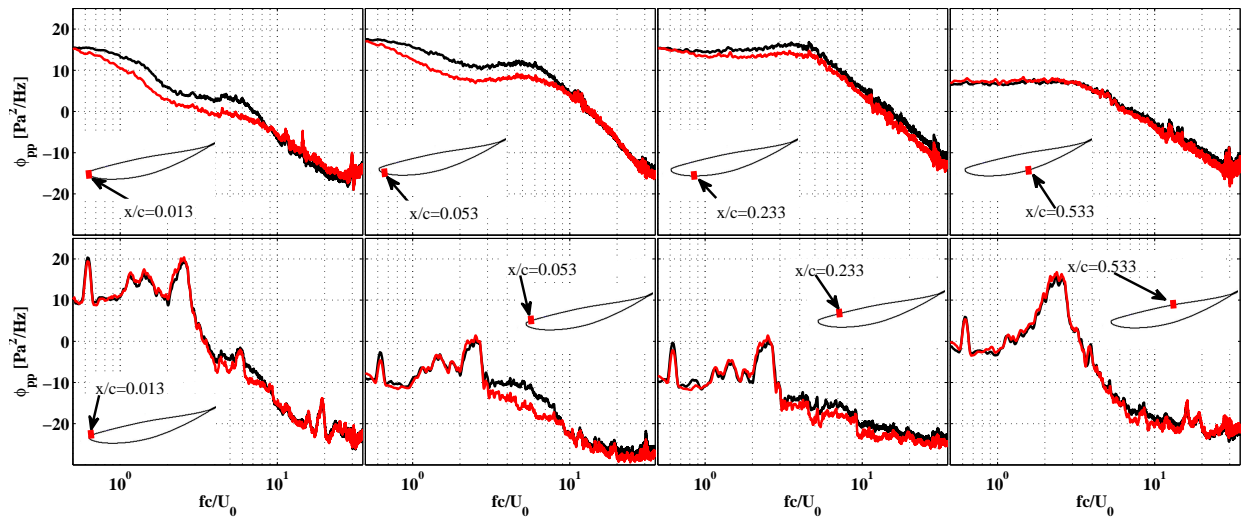
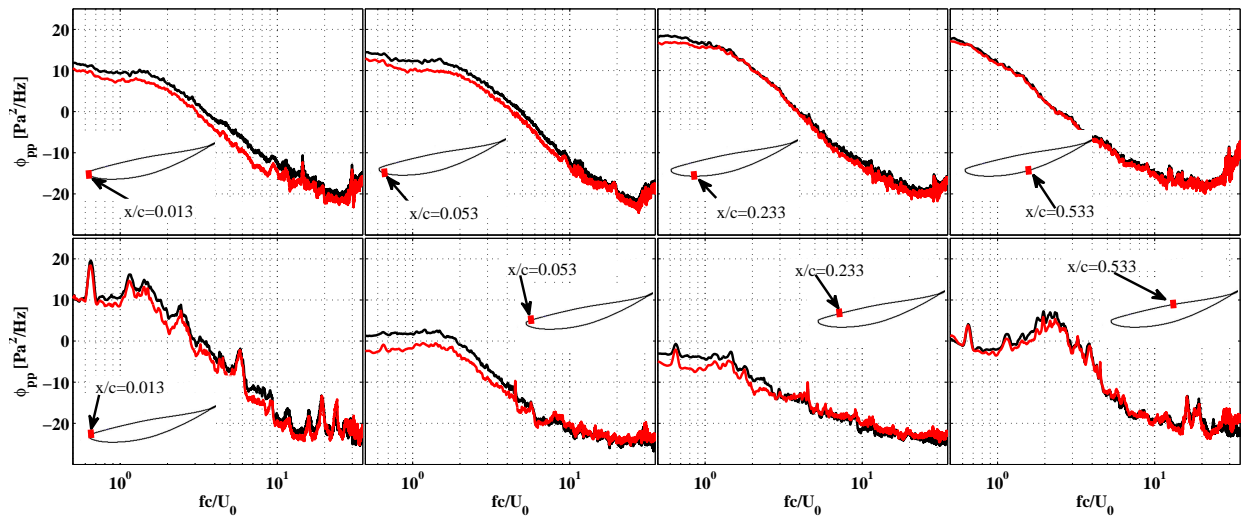(c) Gap distance between the airfoils, $W = 1.0\ c$

Figure 9: Wake development for NACA 65-710 at $\alpha = 10°$, black line: Baseline, red line: Serrated

(a) Gap distance between the airfoils, $W = 0.3\ c$

(b) Gap distance between the airfoils, $W = 0.5\ c$
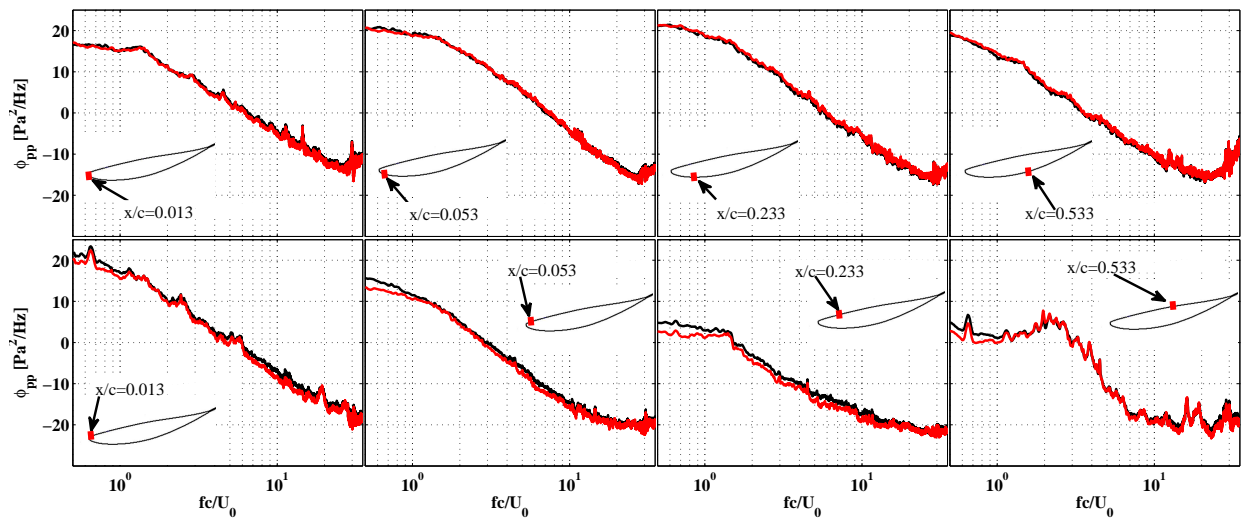

(c) Gap distance between the airfoils, $W = 1.0\ c$

Figure 10: Wake development for NACA 65-710 at $\alpha = 15°$, black line: Baseline, red line: Serrated

References

[1]Hanson D. B. Noise of Counter-Rotation Propellers, *Journal of Aircraft*, **22** (7), 609–617, (1985).

[2]Brooks, T., Pope, D. and Marcolini, M. Airfoil Self-Noise and Prediction, *NASA-RP-1218*, (1989).

[3]Sandberg, R. and Jones, L. Direct numerical simulations of low reynolds number flow over airfoils with trailing-edge serrations, *Journal of Sound and Vibration*, **330** (16), 3818–3831, (2011).

[4]Moreau, D., Brooks, L. and Doolan, C. On the noise reduction mechanism of a flat plate serrated trailing edge at low-to-moderate reynolds number, *18th AIAA/CEAS aeroacoustics conference (33rd AIAA aeroacoustics conference)*, (AIAA 2012-2186).

[5]Chong, T., Joseph, P. and Gruber, M. Airfoil self noise reduction by non-flat plate type trailing edge serrations, *Applied Acoustics*, **74** (4), 607–613, (2013).

[6]Ji, L., Qiao, W., Tong, F., Xu, K. and Chen, W. Experimental and numerical study on noise reduction mechanisms of the airfoil with serrated trailing edge, *20th AIAA/CEAS Aeroacoustics Conference*, (AIAA 2014-3297).

[7]Liu, X., Azarpeyvand, M. and Theunissen, R. Aerodynamic and aeroacoustic performance of serrated airfoils, *21st AIAA/CEAS Aeroacoustics Conference*, (AIAA 2015-2201).

[8]Liu, X., Azarpeyvand, M. and Theunissen, R. On the aerodynamic performance of serrated airfoils, *22nd International Congress on Sound and Vibration*, pp. 12–16, (2015).

[9]Liu, X., Kamliya Jawahar, H., Azarpeyvand, M. and Theunissen, R. Wake development of airfoils with serrated trailing edges, *22nd AIAA/CEAS Aeroacoustics Conference*, (AIAA 2016-2817).

[10]Avallone, F., Arce Leon, C., Pröbsting, S., Lynch, K. P. and Ragni, D. Tomographic-PIV investigation of the flow over serrated trailing-edges, *54th AIAA Aerospace Sciences Meeting*, (AIAA 2016-1012).

[11]Chong, T. P. and Joseph, P. F. An experimental study of airfoil instability tonal noise with trailing edge serrations, *Journal of Sound and Vibration*, **332** (24), 6335–6358, (2013).

[12]Azarpeyvand, M., Gruber, M. and Joseph, P. An analytical investigation of trailing edge noise reduction using novel serrations, *19th AIAA/CEAS aeroacoustics conference*, (AIAA 2013-2009).

[13]Gruber, M. Airfoil noise reduction by edge treatments, *Thesis, University of Southampton*, (2012).

[14]Gruber, M., Azarpeyvand, M. and Joseph, P. F. Airfoil trailing edge noise reduction by the introduction of sawtooth and slitted trailing edge geometries, *integration*, **10**, 6, (2010).

[15]Gruber, M., Joseph, P. and Azarpeyvand, M. An experimental investigation of novel trailing edge geometries on airfoil trailing edge noise reduction, *19th AIAA/CEAS Aeroacoustics Conference*, (A1AA 2013-2011).

[16]Vathylakis, A., Chong, T. P. and Joseph, P. F. Poro-serrated trailing-edge devices for airfoil self-noise reduction, *AIAA Journal*, **53** (11), 3379–3394, (2015).

[17]Showkat Ali, S. A., Szoke, M., Azarpeyvand, M. and Ilário, C. Trailing edge bluntness flow and noise control using porous treatments, *22nd AIAA/CEAS Aeroacoustics Conference*, (AIAA 2016-2832).

[18]Showkat Ali, S. A., Liu, X. and Azarpeyvand, M. Bluff body flow and noise control using porous media, *22nd AIAA/CEAS Aeroacoustics Conference*, (AIAA 2016-2754).

[19]Showkat Ali, S. A., Azarpeyvand, M., da Silva and Ilário, C. Boundary layer interaction with porous surface and implications for aerodynamic noise, *23rd International Congress on Sound & Vibration*, (ICSV 2016).

[20]Afshari, A., Azarpeyvand, M., Dehghan, A. A. and Szoke, M. Trailing edge noise reduction using novel surface treatments, *22nd AIAA/CEAS Aeroacoustics Conference*, (AIAA 2016-2384).

[21]Afshari, A., Dehghan, A. A., Azarpeyvand, M. and Szőke, M. Three-dimentional surface treatments for trailing edge noise reduction, *22nd AIAA/CEAS Aeroacoustics Conference*, (AIAA 2016-2384).

[22]Herr, M. and Dobrzynski, W. Experimental investigations in low-noise trailing edge design., *AIAA journal*, **43** (6), 1167–1175, (2005).

[23]Finez, A., Jacob, M., Jondeau, E. and Roger, M. Broadband noise reduction with trailing edge brushes, *16th AIAA/CEAS Aeroacoustics Conference*, (AIAA 2010-3980).

[24]Ai, Q., Azarpeyvand, M., Lachenal, X. and Weaver, P. M. Aerodynamic and aeroacoustic performance of airfoils with morphing structures, *Wind Energy*, (Vol. 19, No. 7, 2016, pp. 1325-1339).

[25]Ai, Q., Azarpeyvand, M., Lachenal, X. and Weaver, P. M. Airfoil noise reduction using morphing trailing edge, *21st International Congress on Sound and Vibration*, (2014).

[26]Howe, M. S. A Review of the Theory of Trailing Edge Noise, *Journal of Sound and Vibration*, **61** (3), 437–465, (1978).

[27]Howe, M. S. Noise Produced by a Sawtooth Trailing Edge, *Journal of the Acoustical Society of America*, **90** (1), 482–487, (1991).

[28]Howe, M. S. Aerodynamic Noise of a Serrated Trailing Edge, *Journal of Fluids and Structures*, **5** (1), 33–45, (1991).

[29]Lyu, B., Azarpeyvand, M. and Sinayoko, S. A Trailing-Edge Noise Model for Serrated Edges, *AIAA Paper 2015-2362*, (2015).

[30]Lyu, B., Azarpeyvand, M. and Sinayoko, S. Prediction of Noise from Serrated Trailing-Edges, *Journal of Fluid Mechanics*, **793**, 556–588, (2016).

[31]Liu, X., Kamliya Jawahar, H., Azarpeyvand, M. and Theunissen, R., Aerodynamic performance and wake development of airfoils with serrated trailing-edges, *AIAA journal*, (Manuscript Under Review, 2017).